Transcriptomic Profiling of Plaque Psoriasis and Cutaneous T-Cell Subsets during Treatment with Secukinumab

Jared Liu[1], Hsin-Wen Chang[1], Robby Grewal[1], Daniel D. Cummins[1], Audrey Bui[1], Kristen M. Beck[2], Sahil Sekhon[3], Di Yan[4], Zhi-Ming Huang[1], Timothy H. Schmidt[1], Eric J. Yang[5], Isabelle M. Sanchez[6], Mio Nakamura[7], Shrishti Bhattarai[1], Quinn Thibodeaux[1], Richard Ahn[8], Mariela Pauli[1], Tina Bhutani[1], Michael D. Rosenblum[1] and Wilson Liao[1]

The IL-17A inhibitor secukinumab is efficacious for the treatment of psoriasis. To better understand its mechanism of action, we investigated its impact on psoriatic lesions from 15 patients with moderate-to-severe plaque psoriasis undergoing secukinumab treatment. We characterized the longitudinal transcriptomic changes of whole lesional skin tissue as well as cutaneous CD4+ and CD8+ T effector cells and CD4+ T regulatory cells across 12 weeks of treatment. Secukinumab was clinically effective and reduced disease-associated overexpression of *IL17A, IL17F, IL23A, IL23R*, and *IFNG* in whole tissue as soon as 2 weeks after initiation of treatment. *IL17A* overexpression in T-cell subsets, primarily CD8+ T cells, was also reduced. Although secukinumab treatment resolved 89–97% of psoriasis-associated expression differences in bulk tissue and T-cell subsets by week 12 of treatment, we observed expression differences involved in IFN signaling and metallothionein synthesis that remained unresolved at this time point as well as potential treatment-associated expression differences involved in IL-15 signaling. These changes were accompanied by shifts in broader immune cell composition on the basis of deconvolution of RNA-sequencing data. In conclusion, our study reveals several phenotypic and cellular changes within the lesion that underlie clinical improvement from secukinumab.

INTRODUCTION

Psoriasis is a chronic inflammatory skin disease affecting about 2% of the population (Lebwohl, 2003). This disease primarily manifests as scaly, epidermal lesions formed by a hyperproliferation of abnormally differentiating keratinocytes and an infiltration of activated innate and adaptive immune cells. These pathological changes are currently understood to result from an immune-mediated response to autoantigens whose diversity and pathogenic origins are still largely unknown.

The cytokine IL-17A has been found to drive much of the cellular pathology of psoriasis. It is produced by a number of infiltrating immune cell types, including T cells, neutrophils, and mast cells, in psoriatic lesions (Brembilla et al., 2017; Lowes et al., 2008; Reich et al., 2015), where it induces proliferation, hinders differentiation, and upregulates the expression of inflammatory cytokines in keratinocytes (Lai et al., 2012; Teunissen et al., 1998), thereby promoting and maintaining the characteristic physiopathology of psoriasis.

Supporting a central role for IL-17A in psoriasis is the success of the IL-17A blocker secukinumab in the treatment of this disease. Secukinumab was found to be efficacious in the treatment of psoriasis in two major phase 3 clinical trials, reducing PASI scores, a measure of disease severity, by 75% in over 70% of patients with psoriasis, higher than the response rate achieved by the TNF blocker etanercept (Langley et al., 2014). At the transcriptomic level, clinical improvement in response to secukinumab was found to correlate with a resolution of disease-associated gene expression (i.e., genes differentially expressed [DE] between pretreatment psoriatic skin and healthy skin) in lesional tissue, notably in genes involved in T helper (Th) 17 signaling and development, such as *IL17A, IL23A*, and *IFNG* (Hueber et al., 2010; Krueger et al., 2019).

Presently, it is still unclear how secukinumab affects specific resident cell types in the lesion, particularly T cells,

[1]Department of Dermatology, University of California San Francisco, San Francisco, California, USA; [2]Department of Dermatology, UT Southwestern Medical Center, Dallas, Texas, USA; [3]Department of Dermatology, Howard University, Washington, District of Columbia, USA; [4]The Ronald O. Perelman Department of Dermatology, NYU Grossman School of Medicine, NYU Langone Health, New York, New York, USA; [5]Department of Dermatology, The Warren Alpert Medical School of Brown University, Providence, Rhode Island, USA; [6]Department of Dermatology, College of Medicine, University of Illinois, Chicago, Illinois, USA; [7]Department of Dermatology, Michigan Medicine, University of Michigan, Ann Arbor, Michigan, USA; and [8]Institute for Quantitative & Computational Biosciences, University of California Los Angeles, Los Angeles, California, USA

Correspondence: Wilson Liao, Department of Dermatology, University of California San Francisco, 2340 Sutter Street, Box 0808, San Francisco, California 94143, USA. E-mail: wilson.liao@ucsf.edu

Abbreviations: CD8, CD8+ effector T cell; DE, differentially expressed; FDR, false discovery rate; PCA, principal component analysis; PGA, Physician's Global Assessment; RNA-seq, RNA sequencing; Teff, effector T cell; Th, T helper; Treg, regulatory T cell

Received 4 April 2021; revised 3 July 2021; accepted 29 July 2021; accepted manuscript published online 30 December 2021; corrected proof published online 15 March 2022

Cite this article as: JID Innovations 2022;2:100094

Figure 1. Study design and clinical results. (**a**) Study timeline. (**b**) Clinical improvement in two representative patients responding to secukinumab.
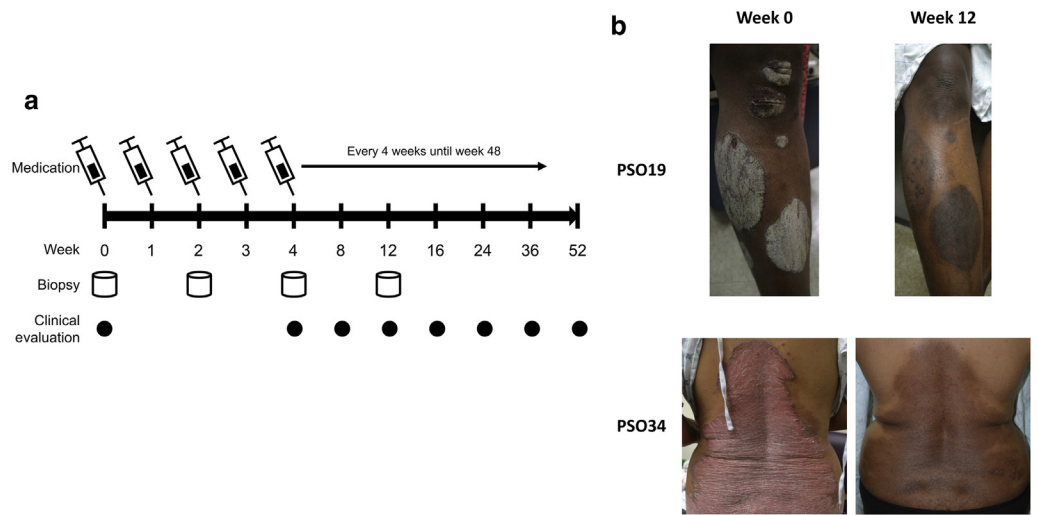
which are currently understood to play an important initiating role in psoriasis within the context of IL-17A signaling. Th17 cells and Tc17 cells occur at higher frequency in psoriatic lesions than in healthy skin (Liu et al., 2021; Lowes et al., 2008), and several identified psoriasis autoantigens, such as LL37 (Lande et al., 2014) and the melanocyte protein ADAMTSL5 (Arakawa et al., 2015), have been found to activate T cells to produce IL-17A.

In this study, we used RNA sequencing (RNA-seq) to characterize the longitudinal response of lesional CD4+ effector T cell (Teff), CD8+ effector T cell (CD8), and CD4+ regulatory T cell (Treg) subsets as well as whole tissue to secukinumab treatment, focusing on alterations in genes, pathways, and cellular composition under disease and treatment conditions.

RESULTS

We characterized the clinical and molecular responses of 15 patients with psoriasis who received secukinumab (300 mg) throughout the 52-week study interval (Figure 1a). The patient demographics are summarized in Table 1. The median age of the participants was 37 years, 60% were male, and the mean duration of psoriasis was approximately 15 years. The mean PASI score was 20.8, and 80% of the patients had a baseline Physician's Global Assessment (PGA) score of 4 or 5. A majority (87%) of participants had previously been treated with either phototherapy, conventional systemic therapy, or biologic therapy. Additional patient information is included in Supplementary Table S1. Of the total 15 patients enrolled, 13 patients completed all the 52 weeks of the study because one patient was lost to follow-up after week 36, and another was discontinued from the study owing to a neurologic event after week 24, which was thought to be unrelated to the study treatment.

Clinical improvement in response to secukinumab

Clinical measures of psoriasis severity improved in response to secukinumab. At week 12, plaques were substantially reduced (Figure 1b), and 100% of patients achieved PASI75, indicating a 75% or greater reduction in disease severity, with 38% achieving PASI90. In terms of the speed of response, the cumulative mean reduction in PASI at weeks 4, 8, and 12 was 65, 86, and 90%, respectively. The mean PGA of patients was 4.0 at week 0 and 1.3 at week 12 (Table 2). PASI and PGA remained decreased until week 36 for most patients, with six patients showing an increase in PASI and PGA at week 52 during the period where secukinumab administration was not directly observed. Of the patients with reduced PASI at week 52, three were observed to respond rapidly to treatment, achieving PASI100 at week 8 and remaining at PASI100 for all subsequent evaluations.

Whole skin and CD8+ T-cell–specific downregulation of *IL17* and *IL23* gene expression in response to secukinumab

To investigate the transcriptomic response to secukinumab, we biopsied lesional skin from patients with psoriasis before treatment and at weeks 2, 4, and 12 of treatment for comparison with skin biopsies from 13 healthy subjects. We performed RNA-seq on bulk skin tissue as well as on CD8+ T cells, Teffs, and Tregs sorted from these biopsies, sequencing each sample to an average depth of 41 million reads per sample. Of the 271 collected samples, 241 (89%) passed quality control, providing 9–14 samples per cell type per time point for analysis.

Within lesional skin, psoriasis-associated inflammatory gene expression was largely normalized during the course of secukinumab treatment. *IL17A*, *IL17F*, and *IL23A*, along with the genes encoding their major receptors *IL17RA*, *IL17RC*, *IL23R*, and *IL12RB1*, were upregulated in untreated lesional skin relative to those in the healthy skin (Figure 2a). These differences were either significant or trended toward significance (e.g., false discovery rate [FDR]-adjusted *P*-values of 0.059 and 0.085 for *IL17A* and *IL23R*, respectively). By week 12 of treatment, the expression of these genes had decreased to levels that were not significantly different from those of the healthy samples. Disease-associated upregulation of *IFNG* was also reversed with treatment, but no significant disease- or treatment-related changes were observed in the expression of *TNF*, consistent with the modest changes observed in a previous study (Hueber et al., 2010).

Among lesional T-cell subsets, only CD8+ T cells expressed significantly elevated *IL17A* (Figure 2b), and by week 12 of

Table 1. Patient Characteristics

Characteristic	Patients (n = 15)
Median age, y	37
Male sex, n (%)	9 (60)
Race/ethnicity, n (%)[1]	
Asian/Pacific Islander	4 (27)
Black/African American	2 (13)
Caucasian	5 (33)
Hispanic	4 (27)
Duration of psoriasis, y	15 (±10)
PASI score	20.8 ± 13.4
PGA score, n (%)	
3	3 (20)
4	9 (60)
5	3 (20)
Psoriatic arthritis, n (%)	1 (7)
Family history of psoriasis, n (%)	5 (33)
Previous treatment, n (%)	
Topical therapy only	2 (13)
Phototherapy[2]	9 (60)
Conventional systemic therapy[3]	5 (33)
Biologic agent	9 (60%)

Abbreviation: PGA, Physician's Global Assessment; y, year.

PASI scores range from 0 to 72, with higher scores indicative of more severe disease. PGA evaluates psoriasis on a scale from 0 to 5, with 0 indicating cleared psoriasis, 1 indicating minimal psoriasis, 2 indicating mild psoriasis, 3 indicating moderate psoriasis, 4 indicating marked psoriasis, and 5 indicating severe psoriasis. Plus–minus values are the SDs from the mean.

[1]Race was self-reported.

[2]Phototherapy included UVB therapy and psoralen plus UVA therapy.

[3]Conventional systemic therapies include methotrexate, acitretin, and cyclosporine.

Table 2. Average Clinical Response to Secukinumab

Week	0	4	8	12	16	24	36	52
PASI	20.4	7.1	2.9	2.0	2.2	2.0	2.0	4.9
PGA	4.0	2.7	1.7	1.3	1.3	1.3	1.4	2.0

Abbreviation: PGA, Physician's Global Assessment.

secukinumab treatment, the expression of this gene was again reduced to levels not statistically different from those of the healthy samples. In contrast, psoriatic Teffs and Tregs did not display abnormal differences in *IL17A, IL17F, TNF,* or *IFNG* levels (Figure 2c and d), and expression of these genes in these subsets was not significantly altered by secukinumab.

Global transcriptional profile of secukinumab-treated lesions and T-cell subsets

A more general comparison of expression profiles revealed a broad shift in lesional gene expression over the course of secukinumab treatment. A principal component analysis (PCA) of 25,608 genes detected among the 66 bulk tissue samples showed a marked separation between 14 lesional samples biopsied before treatment and 11 healthy skin samples along the first and second principal components (Figure 3a). Lesional skin biopsied at subsequent weeks of treatment mark a progression toward the 11 healthy samples along principal component 1 but remain largely separate from the healthy samples, even by week 12 of treatment, when most patients had achieved PASI75.

In contrast to the consistent shift in the gene expression seen in bulk lesional tissue, we found more variability among sorted T-cell populations in terms of their transcriptomic profiles and their response to secukinumab. In PCA plots of gene expression profiles from sorted CD8$^+$ T cells, Teffs, and Tregs, we found some separation between healthy and

lesional samples (Figure 3b–d) but no consistent progression during treatment.

Disease-resolving and treatment-associated expression changes in response to secukinumab

Most disease-associated gene expression differences in bulk tissue and sorted cells were resolved during secukinumab treatment. We detected 11–3,096 DE genes among week 0, week 12, and healthy samples (Table 3 and Supplementary Table S3). Of the 3,096 DE genes we found between healthy skin and untreated psoriatic lesions, 2,919 (94%) no longer showed significant differences between healthy skin and psoriatic lesions sampled at week 12 of treatment (Figure 4a). A similar resolution of disease-associated expression differences was found among the sorted T-cell samples, with an average of 94% of DE genes in each subset restored at week 12. The general magnitude of expression differences in these DE genes was also progressively reduced throughout the first 12 weeks of treatment (Figure 4b), indicating reduced disease severity in response to secukinumab that is consistent with the observed clinical improvement mentioned earlier.

At the same time, secukinumab treatment was also associated, to varying extents, with gene expression changes in bulk tissue and T-cell subsets that we had not identified as DE between untreated psoriatic lesions and healthy skin. For instance, within psoriatic lesions at week 12 of treatment, such treatment-associated expression differences were found in 105 genes from bulk tissue, 19 genes in CD8$^+$ T cells, 1,651 in Teffs, and 200 genes in Tregs (Figure 4c and d and Supplementary Table S3). A closer examination of the largest group of treatment-associated DE genes from week 12 in Teffs revealed that it is largely driven by samples from two subjects (Supplementary Figure S1). This could indicate that many of these treatment-associated genes may be due to technical noise or interindividual variation. Excluding the two samples from the analysis of week 12 Teffs produced a much shorter list of 58 treatment-associated expression changes (Supplementary Table S4) that included downregulation of *IL15*. *IL15* and its receptor *IL15RA* similarly showed treatment-associated downregulation in week-2 Treg samples and week-4 Teff samples, respectively (Supplementary Table S3), raising the possibility that IL-15 signaling may be another pathway affected by primary IL-17 signaling blockade from secukinumab.

Disease-associated pathways resolved and unresolved by secukinumab treatment

The DE genes found between untreated psoriasis bulk skin and healthy bulk skin (week 0 vs. healthy) (Figure 5a and c and Supplementary Table S5) represent many pathways important for psoriasis pathogenesis. Psoriatic skin showed higher expression of genes involved in keratinocyte
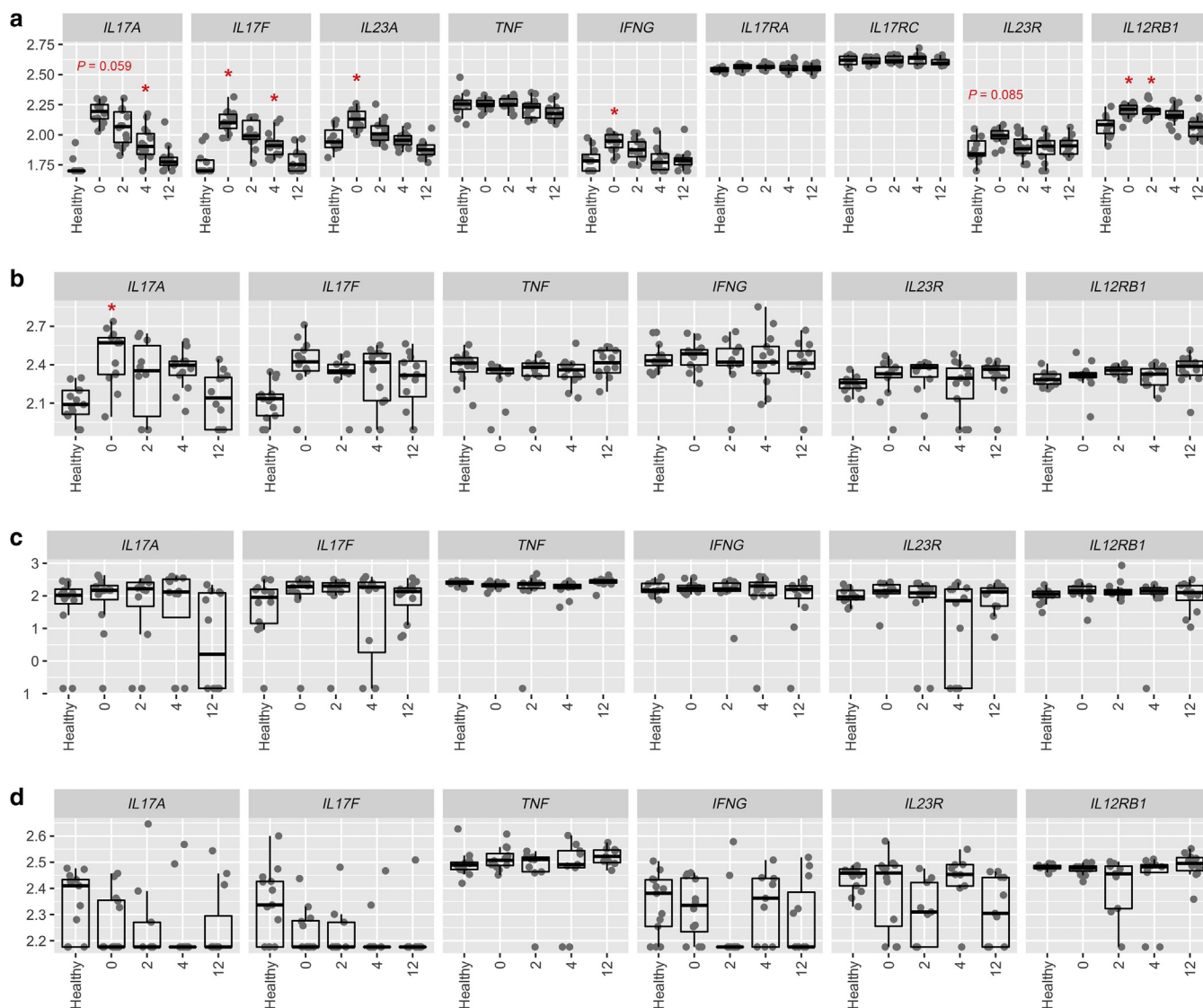
Figure 2. Expression of psoriasis-associated inflammatory genes is reduced in whole tissue and CD8^{+} T cells during secukinumab treatment. DESeq2-normalized and variance-stabilized expression of inflammatory genes in healthy, treated, and untreated samples for (**a**) bulk tissue, (**b**) CD8^{+} T cells, (**c**) Teffs, and (**d**) Tregs. Significance of differences based on Wald tests from separate DESeq2 models calculated between healthy samples and the samples of each time point. Asterisk (*) shows the FDR-adjusted *P* < 0.05. Sample sizes are shown in Supplementary Table S2. FDR, false discovery rate; Teff, effector T cell; Treg, regulatory T cell.

differentiation (FDR = 0.01), epidermis development (FDR = 0.008), and the mitotic cell cycle process (FDR < 10^{18}), consistent with a hyperproliferation of keratinocytes that are characteristic of psoriasis. Granulocyte activation genes (FDR = 0.0003), specifically of neutrophils (FDR = 0.0003), are also overrepresented, supporting the current understandings of the pathogenic role this immune cell type plays in psoriatic skin (Chiang et al., 2019). Finally, IFN-γ (FDR = 0.03), IL-17 (FDR = 0.003), and IL-23 (FDR = 0.02) signaling pathways are also enriched among the DE genes upregulated in psoriasis skin.

Conversely, the genes that are downregulated in psoriasis skin compared with those in healthy skin (Figure 5b and c and Supplementary Table S5) contain an overrepresentation of genes involved in negative regulation of locomotion (FDR = 0.01), MAPK signaling (FDR = 0.01), and extracellular signal–regulated kinase signaling (FDR = 0.007),

consistent with increased migration and activation of T cells commonly observed in psoriatic skin. Downregulated genes were also involved in negative regulation of fat cell differentiation (FDR = 0.02) and zinc ion homeostasis (FDR = 0.04), the last category including genes such as *MT1A, MT2A, MT1E, MT1M,* and *MT1X* that encode metallothioneins, which are small, ubiquitous, cysteine-rich proteins with antioxidant properties that have been implicated in mediating anti-inflammatory effects in various mouse models (Inoue et al., 2009).

Within T-cell subsets, DE genes between psoriatic and healthy skin generally reflected the differences in immune signaling and activation. The top 10 most overrepresented pathways in CD8s largely consisted of genes within the chemokine-mediated signaling pathway (FDR = 0.02), such as *CXCL1, CXCL2,* and *CXCL8,* as well as genes involved in inflammatory responses (FDR = 0.005), endothelium
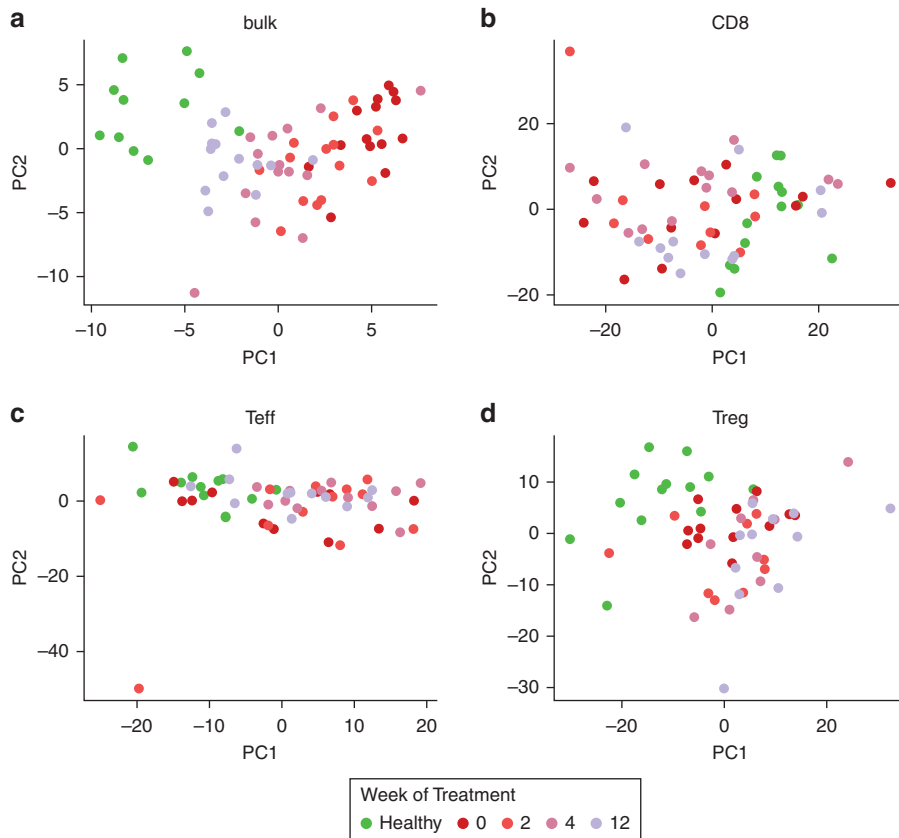
Figure 3. Broad shifts in lesional gene expression in response to secukinumab. PCA plots of (**a**) bulk tissue, (**b**) CD8s, (**c**) Teffs, and (**d**) Tregs. PCA was performed on normalized expression data from healthy, treated, and untreated samples of each sample type that were adjusted for the estimated effects of technical variables and variance stabilized. Sample sizes are shown in Supplementary Table S2. CD8, CD8+ effector T cell; PC, principal component; PCA, principal component analysis; Teff, effector T cell; Treg, regulatory T cell.

development (FDR = 0.03), and cell migration (FDR = 0.03), such as *GJA1, STC1, CLIC4,* and *CAV1* (Supplementary Table S3 and S5). These genes in particular were also DE by Teffs in psoriatic compared with those in healthy skin and appear in many of the top 10 most overrepresented pathways in this subset as well. In both CD8s and Teffs, most DE genes involved in inflammatory signaling, including the common genes mentioned earlier, were downregulated in psoriatic skin with notable exceptions, namely *IL17A* in CD8s and the cytolytic gene *GNLY* and chemokine *CXCL13* in Teffs. Although no overrepresented biological processes or pathways were found among DE genes from psoriatic Tregs compared with those from their healthy counterparts, a similar downregulation of inflammatory signaling genes such as *CXCL2, CXCL3,* and *CCL22* was observed in this subset.

Some of the major biological processes identified among the disease-associated DE genes from bulk tissue and T-cell subsets are also represented in the small set of genes that remain unresolved after 12 weeks of secukinumab treatment.

In bulk tissue, the downregulation of metallothionein genes along with upregulation of several IFN-induced genes (such as *OAS1, OAS2, OAS3, IFI2,* and *IFI3*) persisted as unresolved disease perturbations at or through week 12 of secukinumab treatment (Supplementary Table S3 and S5), representing the pathogenic processes that potentially occur independently of or distantly from IL-17 blockade. Unresolved week-12 expression changes in T-cell subsets included the downregulation of the cytokines *IL2* and *CXCL8* along with the metallothionein *MT1A* in CD8s and upregulation of *GNLY* in Teffs (Supplementary Table S3).

Psoriasis-associated increases in lesional Treg population are reduced by secukinumab

To investigate whether the gene expression changes within T-cell subsets reported earlier are accompanied by changes in T-cell subset composition and inflammatory potential, we performed flow cytometric analysis on the same samples used for RNA-seq. Healthy skin and untreated lesions showed comparable proportions of CD8s and Teffs;

Table 3. Differentially Expressed Genes between Healthy, Untreated, and Treated Samples

| Sample Type	Week 0 Versus Healthy Up/Down	Week 0 Versus Week 12 Up/Down	Week 12 Versus Healthy Up/Down
Bulk	1289/1807	900/1165	96/186
CD8+ T cell	40/89	2/26	7/18
Teff	9/28	3/11	1556/99
Treg	13/62	22/17	76/126

Abbreviations: Teff, effector T cell; Treg, regulatory T cell.
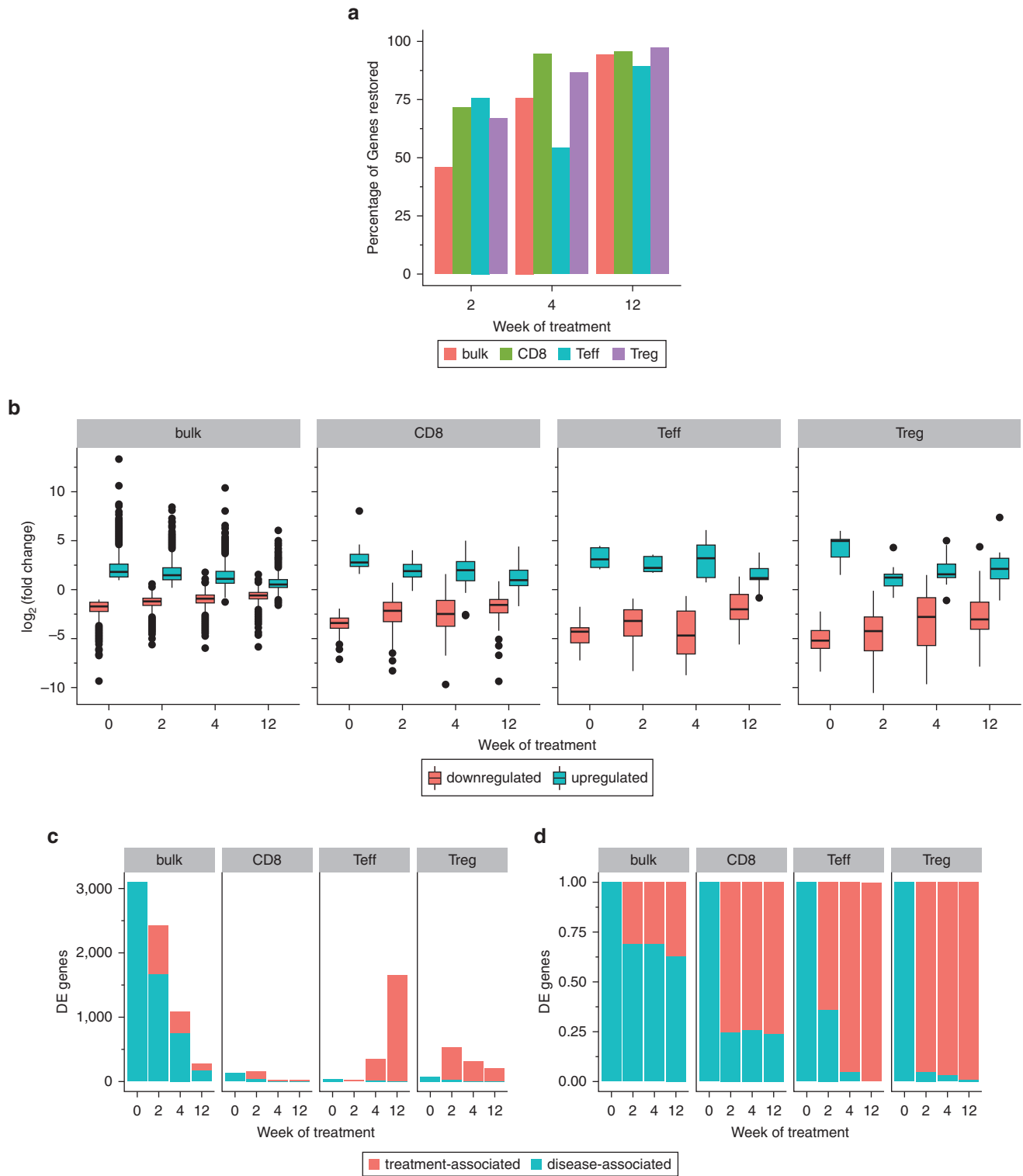
Figure 4. Secukinumab restores disease-associated transcriptomic changes and leads to treatment-associated expression differences. (**a**) Percentage of DE genes between healthy skin and untreated psoriatic lesion samples resolved at each time point of treatment. (**b**) Log fold changes of these genes at each time point, which have been classified as upregulated or downregulated on the basis of their $\log_2$ fold change between psoriatic and healthy samples. (**c**) Number and (**d**) percentage of disease-associated or treatment-associated DE genes at each time point. CD8, CD8^{+} effector T cell; DE, differentially expressed; Teff, effector T cell; Treg, regulatory T cell.

however, psoriasis lesions contained a significantly higher proportion of Tregs among both CD4^{+} cells and total CD3^{+} cells (Figure 6a), consistent with previous work (Sanchez Rodriguez et al., 2014).

Although Th17-skewed Tregs have been documented to occur in psoriasis lesions (Sanchez Rodriguez et al., 2014), cytokine profiling of stimulated Treg samples in our cohort did not reveal differences in the proportions of Tregs
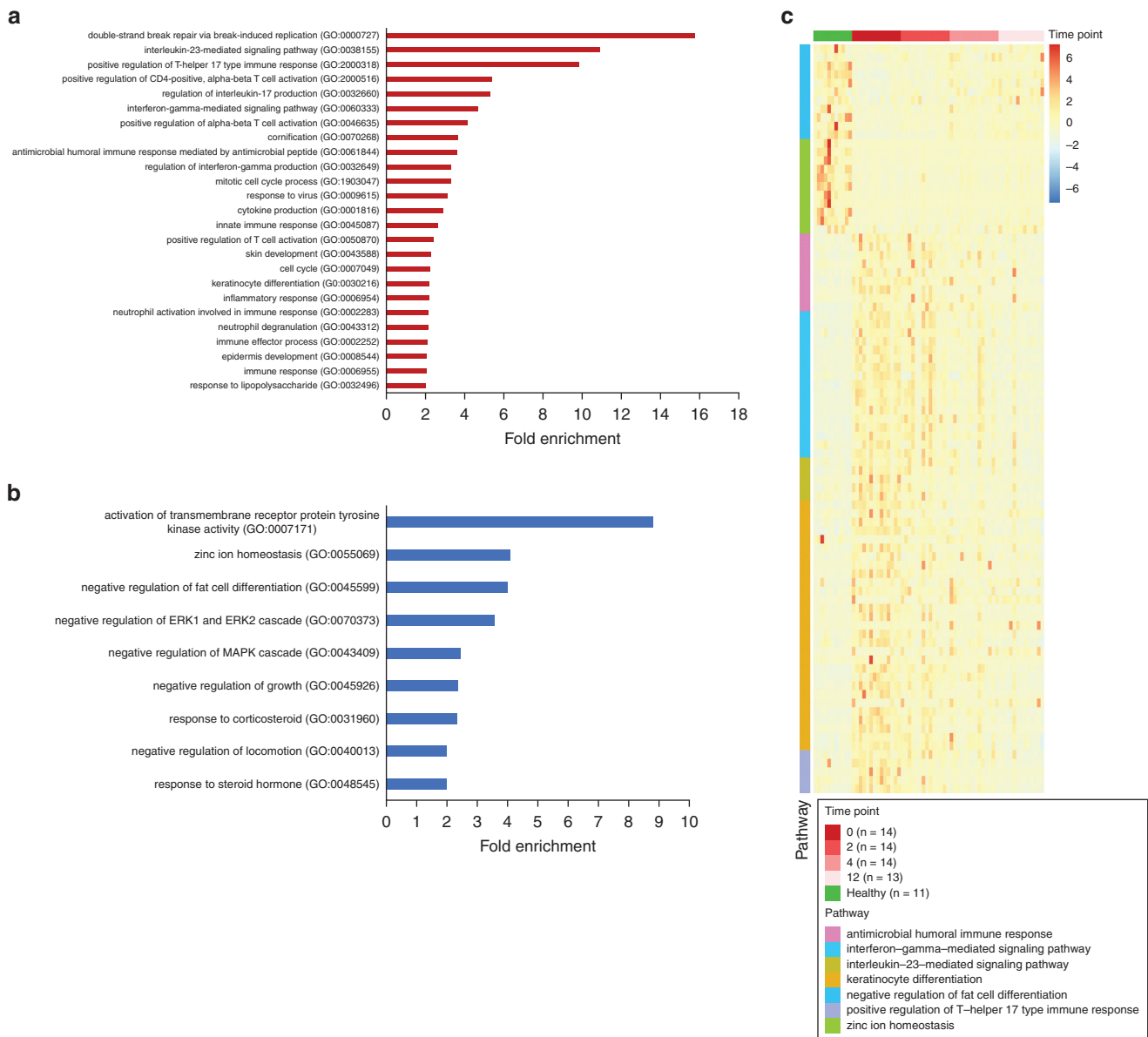
Figure 5. Pathways overrepresented between psoriatic and healthy skin. GO pathways overrepresented among the (**a**) upregulated and (**b**) downregulated DE genes between psoriatic and healthy bulk tissue. (**c**) Normalized, variance-stabilized expression of genes in each pathway across treatment time points. DE, differentially expressed; GO, Gene Ontology.

expressing the Th1/Th17 cytokines IFN-γ, IL-17A, or TNF-α. However, within stimulated CD8s and Teffs, we observed significant increases in cells expressing either IFN-γ, IL-17A, or both within the lesion as well as reduced expression of the Th2 cytokine IL-13 in Teffs (Figure 6b), suggesting a Th1-/Th17-skewed inflammatory potential within these subsets, consistent with findings of previous studies (Cheuk et al., 2014). Although secukinumab treatment did not significantly alter the proportions of cytokine-producing cells in any subset (Supplementary Figure S2), we observed a gradual decrease in Treg proportion that reached significance at week 12 of treatment (Figure 6c).

We expanded our investigation of cell population shifts to the broader immune infiltrate within the lesions before and after treatment by performing deconvolution of RNA-seq expression data from each time point using gene signatures

for 22 immune cell types. The relative abundances of each immune cell type estimated by this analysis were again mostly comparable between healthy skin and psoriatic lesions except for activated memory Teffs, which were increased in psoriatic lesions (Figure 6d). However, secukinumab treatment led to a significant reduction in the proportion of activated memory Teffs by weeks 4 and 12, along with a slight but significant increase in the proportion of Tregs (Figure 6e). Transient increases in M2 macrophages, activated gamma-delta T cells, and plasma cells were also observed at week 4 (Figure 6e).

TCR clonotype analysis identifies TCR sharing between subjects with psoriasis and between T-cell subsets
Finally, we investigated whether secukinumab affects the clonal composition of each T-cell subset using the reads
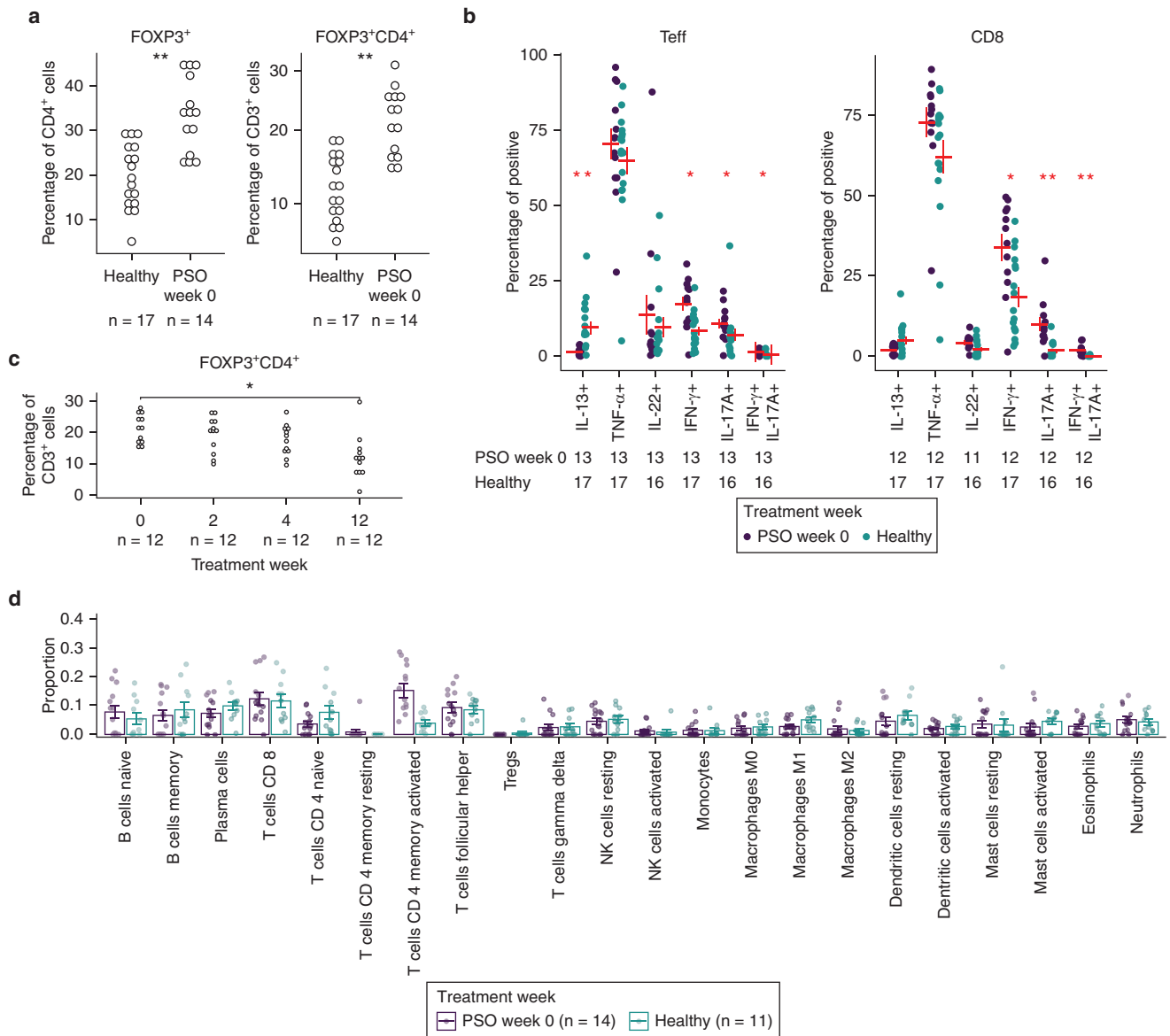
Figure 6. T-cell composition and phenotypic differences before and during secukinumab treatment. (a) Percentage of FOXP3$^+$ cells within sorted CD4$^+$ (left) and CD3$^+$ (right) populations. (b) Percentage of stimulated Teffs (left) and CD8s (right) expressing various inflammatory cytokines. Horizontal bars denote means, and vertical bars denote SEM. (c) Percentage of FOXP3$^+$ cells in sorted CD3$^+$ population from samples taken at weeks 0, 2, 4, and 12 of secukinumab treatment. (d) The predicted proportion of immune cell types within the RNA-seq data of healthy and untreated PSO samples. (e) Changes in predicted proportions of specific immune cell types during secukinumab treatment compared with those in the healthy skin; *$P < 0.05$ and **$P < 0.005$. CD8, CD8$^+$ effector T cell; PSO, psoriatic; RNA-seq, RNA sequencing; Teff, effector T cell; Treg, regulatory T cell.

within each RNA-seq dataset that span the TCR genes *TRA, TRB, TRD,* and *TRG* to survey the clonotype repertoire of psoriatic samples at weeks 0 through 12 of treatment. We detected a median of 125 *TRA,* 187 *TRB,* 125 *TRG,* and 7 *TRD* unique clonotypes within each sample. Both sorted and bulk samples contained similar numbers of *TRA* and *TRB* clonotypes (Figure 7a) despite fewer TCR-spanning reads recovered from bulk samples (Figure 7b), and *TRD* and *TRG* clonotypes were most prominently detected within sorted CD8$^+$ T-cell samples (Figure 7a). Clonal diversity, measured by the number of clonotypes (Figure 7c) as well as the Inverse Simpson Index (Figure 7d), did not significantly change over secukinumab treatment for any TCR locus in either bulk tissue or sorted T cells.

The comparison of TCR repertoires among subjects with psoriasis also identified 1,716 clonotypes shared between at least two subjects with psoriasis but not among healthy subjects (Supplementary Table S6). Most of these psoriasis-specific shared clonotypes consisted of *TRA* sequences (Figure 7e), and comparison of the subject-shared clonotypes with those previously reported to be enriched in psoriasis (Matos et al., 2017) revealed only one common clonotype, TRBV18_CASSPQETQYF_TRBJ2-5. In addition, of the 1,716 clonotypes shared by subjects with psoriasis, 99 were also detected among more than one T-cell subset within the same individual (Supplementary Table S6), supporting the idea that T-cell activity in the lesion involves responses to a common set of antigens by multiple subsets.
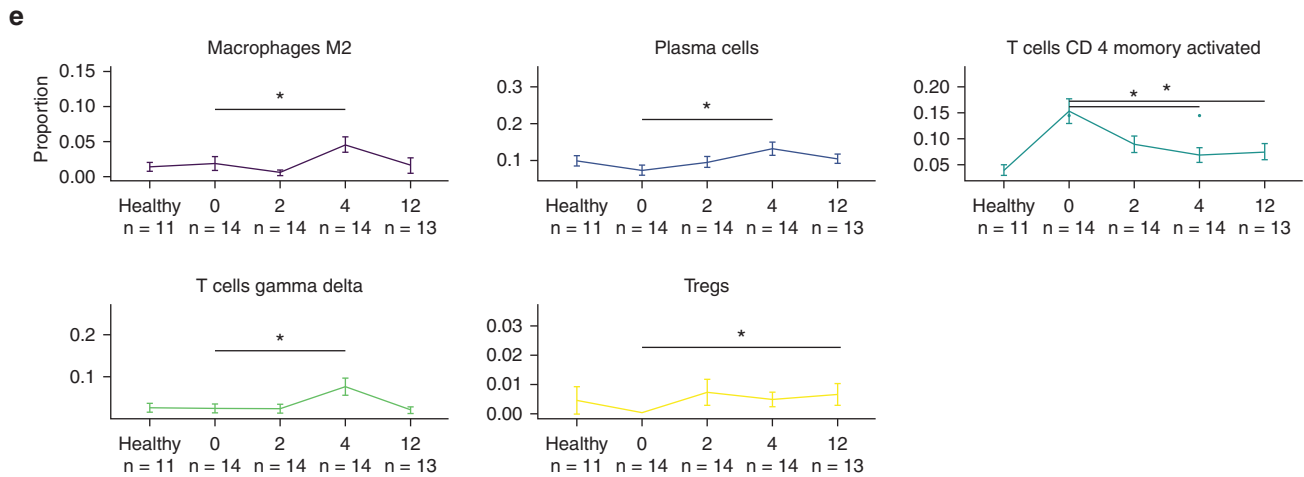
e

Figure 6. Continued.

DISCUSSION

In our study, secukinumab treatment was associated with clinical improvement as well as a general resolution of disease-associated gene expression and pathways in lesional skin, consistent with findings of previous studies (Hueber et al., 2010; Krueger et al., 2019). Although the number of patients in our study was too limited to compare treatment outcomes, our data nevertheless yielded several observations of the lesional response to secukinumab treatment.

First, although secukinumab treatment largely resolved most gene expression differences between healthy and psoriatic skin, a small set of genes involved in cytokine signaling and inflammatory responses outside of IL-17 signaling (e.g., *CXCL1, CXCL2,* and *CXCL8*) remained persistently underexpressed in psoriatic CD8s and Teffs after 12 weeks of secukinumab treatment. These unresolved expression differences could represent durable priming of lesional Teffs and CD8s toward a Th17/Tc17 phenotype, which is supported by the unresolved increase in lesional T cells with IL-17A–producing potential that we observed in our flow cytometry results up to 12 weeks of treatment and is consistent with findings of previous studies showing residual IL-17 and IL-22 production in the T cells of the skin from individuals whose psoriasis was resolved with phototherapy or anti-TNF treatment with etanercept (Matos et al., 2017) as well as anti–IL-12/23 treatment with ustekinumab (Cheuk et al., 2014). Further investigation of these lasting phenotypic T-cell changes, along with the perturbations in IFN signaling and metallothionein expression in lesional skin that we observed to remain unresolved by secukinumab, may yield further strategies for improving the efficacy of this biologic.

Second, although it is generally understood that both CD4$^+$ and CD8$^+$ T cells can produce IL-17 in psoriatic lesions (Lowes et al., 2008; Ortega et al., 2009) and respond to autoantigens (Lande et al., 2014), our study found *IL17A* overexpression and suppression by secukinumab to be more prominent in psoriatic CD8$^+$ T cells rather than in CD4$^+$ T cells. This raises the possibility that CD8$^+$ T cells may contribute to lesional IL-17 signaling more through increased cytokine production in activated cells than through increased numbers of activated cells, the latter possibly applying more

to Teffs on the basis of our RNA-seq deconvolution results. In contrast, the upregulation of *GNLY* in Teffs may indicate the involvement of cytotoxic CD4$^+$ T cells in psoriasis. Although rare in healthy individuals, this subset has been found to occur in certain viral infections (Chemin et al., 2019) and autoimmune conditions such as systemic sclerosis (Maehara et al., 2020) and rheumatoid arthritis (Broadley et al., 2017). The upregulation of *CXCL13* in this subset also suggests that Teffs may be a significant source of this chemokine, which we found in previous work to be characteristic of *IL17A*-expressing CD8s (Liu et al., 2021). These findings warrant further investigation to validate these properties of lesional T cells, especially within the context of other infiltrating, IL-17A–expressing immune cell types.

Third, both bulk tissue and T-cell subsets exhibited secukinumab treatment–associated expression changes, including the downregulation of IL-15 signaling in Teffs and Tregs. Because IL-15 may act upstream of IL-17 signaling (Colpitts et al., 2015; Halvorsen et al., 2011) and has been found to be involved in psoriasis (Villadsen et al., 2003; Zhang et al., 2007), our result potentially suggests an indirect modulation of this pathway in T cells by secukinumab. These and other treatment-associated expression differences may also represent the activation of additional genes and pathways involved in lesion resolution. Additional studies validating and characterizing the impact of IL-17 blockade on IL-15 signaling may reveal further insights into the regulatory relationship between these pathways.

Finally, although we found no clear evidence for whether T-cell clonal diversity responds to treatment (possibly owing to limited sampling of the TCR repertoire), deconvolution of our RNA-seq data suggests that the abundance of specific immune populations, including Teffs and Tregs, may change between weeks 4 and 12 of treatment. We note that although the RNA-seq deconvolution results suggest an increasing relative abundance of Tregs over the course of secukinumab treatment, flow cytometric estimates of Treg proportions suggest a decrease. This may well reflect inherent challenges in interpreting compositional data as well as a lack of correlation between RNA- and protein-level expression of markers used to define Tregs, but whether this subset is
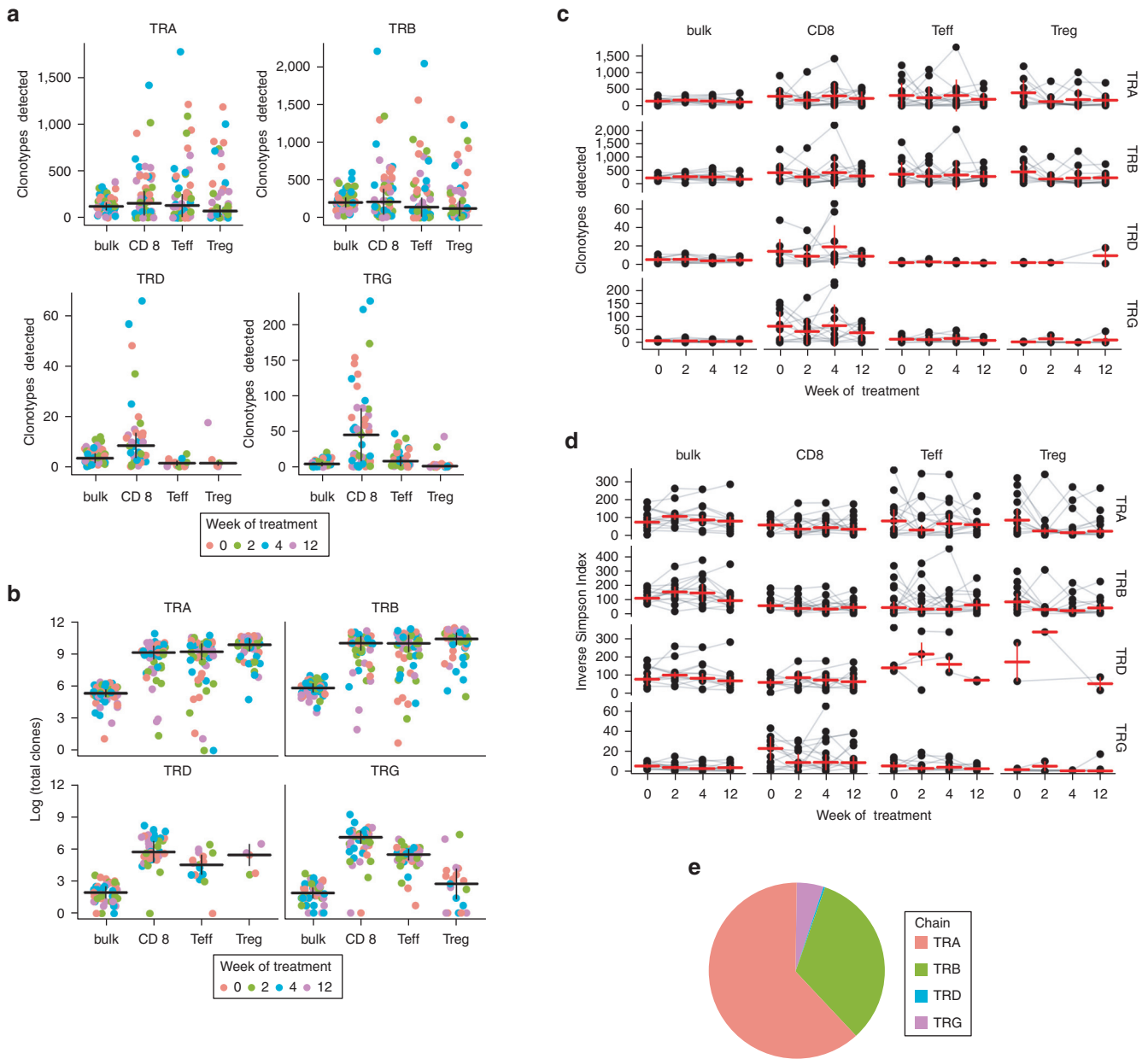
Figure 7. TCR clones and clonotypes recovered from sorted and bulk samples. (**a**) Total clonotypes detected for each locus. (**b**) Total clones (i.e., high-quality TCR-spanning reads) in each sample. (**c**) The number of unique clonotypes and (**d**) inverse Simpson diversity measures for each sample from patients with psoriasis before and during secukinumab treatment, with lines connecting samples from the same subject. (**e**) TCR loci of clonotypes shared by subjects with psoriasis (total = 1,716). Horizontal bars denote the medians, and vertical bars denote the median absolute deviation. Sample sizes are shown in Supplementary Table 2. CD8, CD8+ effector T cell; Teff, effector T cell; Treg, regulatory T cell.

generally increased or decreased in lesions is also thought to depend on psoriasis subtypes and lesion sites under consideration on the basis of various published studies (Nussbaum et al., 2021). Nevertheless, because Tregs in psoriatic lesions have also been found to be dysfunctional in immunosuppression (Sugiyama et al., 2005) and to possibly contribute to pathogenic IL-17 signaling (Nussbaum et al., 2021; Sanchez Rodriguez et al., 2014), one possible explanation for our results is that although the relative cellular abundance of Tregs (measured through flow cytometry) decreases during secukinumab treatment, Treg immunosuppressive function (measured by RNA-seq) simultaneously improves, as represented by the increased expression of

genes and transcriptional programs that define the Treg signature used in our deconvolution analysis. Because some of the expression changes we observed in Tregs at week 12 of secukinumab treatment involve genes encoding cytokine receptors, such as *IL18R1* and *IL7R*, which have been found to play important roles in Treg development and function (Bayer et al., 2008; Harrison et al., 2015; Waickman et al., 2020), further investigation is needed to determine the relationship between the compositional and functional changes that occur in Tregs within resolving psoriatic lesions.

In conclusion, our study provides additional insight into the longitudinal transcriptomic and cellular changes induced by secukinumab within the psoriatic lesion and its resident

T-cell population and highlights directions of further investigation for better understanding the effects of this biologic as well as the pathogenesis of psoriasis.

MATERIALS AND METHODS

Patients

The University of California San Francisco Institutional Review Board (San Francisco, CA) approved this study. All patients provided written informed consent before enrollment. This study was conducted at a single academic center. Patients were at least aged 18 years with a diagnosis of moderate to severe plaque psoriasis for at least 6 months or longer. Moderate-to-severe psoriasis was defined as a PASI score of 12 or higher and as a PGA score of 3 or higher. Patients could have received previous systemic treatment or phototherapy, including anti-TNF, anti–IL-12/-23, and anti–IL-17 biologic agents; however, a washout period of 2 weeks for topicals and phototherapy, 4 weeks for oral systemic medications, 3 months for most biologics, and 6 months for ustekinumab was required. Study subjects received secukinumab (300 mg, subcutaneously) at weeks 0, 1, 2, 3, and 4, then every 4 weeks thereafter until week 48. Three skin punch biopsies were obtained at each of weeks 0, 2, 4, and 12. Pretreatment biopsies were taken from the edge of a psoriatic plaque, and subsequent biopsies in a given patient were taken from the edge of the same plaque or an adjacent plaque. PASI and PGA assessments were performed at weeks 0, 4, 8, 12, 16, 24, 36, and 52.

Biopsy processing

Skin punch biopsies were immediately stored at 4 °C in a container with sterile gauze and PBS until they were ready to be processed. From the three biopsies obtained for a given subject and time point, half of one biopsy was used for bulk RNA-seq (see the section on sample preparation for RNA-seq). The rest of the biopsies were prepared for sorted T-cell RNA-seq and flow cytometry by first trimming hair and subcutaneous adipose before finely mincing and mixing with digestion buffer composed of collagenase type IV (LS04188; Worthington Biochemical, Lakewood, NJ), DNAse (DN25-1G; Sigma-Aldrich, St. Louis, MO), 10% fetal bovine serum, 1% 4-(2-hydroxyethyl)-1-piperazineethanesulfonic acid, and 1% penicillin/streptavidin in RPMI 1640. After overnight incubation in 5% carbon dioxide, cell suspensions were harvested by vigorously shaking for 30 seconds, followed by centrifugation at 300 r.p.m. for 5 minutes at room temperature (Allegra X-14R Centrifuge, Beckman Coulter, Brea, CA). Cell suspensions were then filtered through a 100-µm nylon mesh (catalog number 22363549; Fisher Scientific, Hampton, NH), and the top layer and pellet were discarded. Cells were centrifuged at 1,500 r.p.m. for 5 minutes at 4 °C (Allegra X-14R Centrifuge, Beckman Coulter), the supernatant was discarded, and cells were counted under a light microscope with trypan blue and partitioned for RNA-seq sort and flow cytometry ($\sim$50,000 cells).

Cell sorting for flow cytometry analyses and RNA-seq

Cells aliquoted for flow cytometry were stimulated and incubated for 4 hours with Cell Stimulation Cocktail 500× (TNB-4975; Tonbo Biosciences, San Diego, CA), followed by staining with surface markers (viability dye Ghost Dye Violet 510, 130870; Tonbo Biosciences) and the following antibodies: anti-hCD3 PerCP (SK7; BioLegend, San Diego, CA), anti-hCD4 phycoerythrin-Texas Red (S3.5; Invitrogen, Waltham, MA), anti-hCD45 allophycocyanin-eFluor 780 (2D1; eBioscience, San Diego, CA), anti-hCD27 allophycocyanin-eFluor 780 (47-0271-82′ eBioscience), and anti-hCD8a eVolve 605 (RPA-T8; eBioscience) for 30 minutes at 4 °C.

Cells were fixed and permeabilized (catalog number 00-5521-00; Invitrogen) and then stained with anti-hFOXP3 eFluor 450 (PCH101; eBioscience) and the cytokine antibody mix (anti–hIL-13 FITC [85BRD; eBioscience], anti–hTNF-α phycoerythrin-Cy7 [MAb11; BD Pharmigen, San Diego, CA], anti–hIL-22 phycoerythrin [142928; R&D Systems, Minneapolis, MN], anti–hIFN-γ Alexa Fluor 700 [4S.B3; BioLegend], and anti–hIL-17A eFluor 660 [eBio64CAP17; eBioscience]). We then performed multiparameter flow cytometry using an LSR Fortessa (BD Biosciences, San Jose, CA) flow cytometer and FlowJo (Tree Star, Ashland, OR) software to subset the leukocyte population into defined T-cell populations (CD4+ Teffs, CD8+ T cells, and CD4+ Tregs) and quantify cytokine production. First, a lymphocyte gate was taken, and then doublets were excluded in the following gate. From there, live CD45+ cells were gated and then CD45+ CD3+ cells, and from here, CD4+ and CD8+ cells could be observed. From the CD4+ gate, FOXP3−CD27− cells were gated and called Teffs, and FOXP3+CD27+ cells were called Tregs. Reported post-sort purity was >90% for all populations.

Cells aliquoted for RNA-seq were processed as mentioned earlier but without stimulation, fixation, permeabilization, or cytokine staining. To distinguish Tregs from Teffs, anti-hCD25 phycoerythrin-Cy7 (560920; BD Pharmigen) was substituted for anti-FOXP3. The cells were sorted into 1× lysis buffer from the SMART-Seq, version 4, Ultra Low Input RNA Kit (catalog number 634894; Takara Bio, Shiga, Japan) and snap-frozen in liquid nitrogen for storage at −80 °C.

Sample preparation for RNA-seq

Bulk RNA was extracted from whole skin tissue using Qiagen RNeasy fibrous tissue mini kit (catalog number 74704; Qiagen, Hilden, Germany). Sequencing libraries were constructed for sorted lymphocyte lysates and for purified RNA extracted from whole skin tissue using the SMART-Seq, version 4, Ultra Low Input RNA Kit (catalog number 634894; Takara Bio). Reverse transcription was performed on poly-adenylated RNA from cell lysate for up to 1,000 cells, followed by second-strand synthesis to make full-length cDNA. cDNA was then later amplified by PCR using cycle numbers determined by cell numbers. Amplified cDNA was purified by AMPure XP beads (Beckman Coulter) and followed by Qubit (Invitrogen) quantification. Sequencing libraries were constructed using the Nextera DNA kit (Illumina, Foster City, CA) with 0.4 ng of amplified cDNA for sorted lymphocytes and 0.3 ng for cDNA synthesized from bulk skin RNA. The sizes of constructed libraries were evaluated by the Illumina Bioanalyzer High Sensitivity DNA Assay to ensure that library sizes range between 300 and 500 bp. The libraries were quantified using NEBNext Library Quant Kit for Illumina (catalog number E7630; New England Biolabs, Ipswich, MA) to ensure that equal molar concentrations of sequenceable libraries were pooled. Sequencing reactions were performed on an Illumina Hiseq4000 with paired-end 150 bp reads. More than 30 million reads were generated per sample.

RNA-seq quality control and data processing

Reads were mapped to the GRCh38 build of the human reference genome provided by the Genome Analysis Toolkit (https://console.cloud.google.com/storage/browser/genomics-public-data/resources/broad/hg38/v0/Homo_sapiens_assembly38.fasta) that was annotated by GENCODE 25 using STAR, version 2.4.2a (Dobin et al., 2013). Picard-tools, version 1.139 (http://broadinstitute.github.io/picard), was used to compile mapping statistics for the resulting alignments, and a table of counts of each gene from each sample

was generated with HTSeq, version 0.6.1p1 (Anders et al., 2015). Samples with <1 million reads, 10,000 detected genes, or 60% mappable reads were excluded. Genes expressed at <5 reads in <20% of samples for each cell type were also excluded from further analysis. We used DESeq2, version 1.18.1 (Love et al., 2014), to normalize read counts for each gene between samples and to generate linear models for differential expression analysis, accounting for technical effects and biological variation using the following formula:

$$\sim batch + \text{ number of genes detected}$$
$$+ \text{ percent uniquely mapped reads} + \text{ treatment time point}$$

Genes DE between groups were calculated with DESeq2 using the Wald test with a parametric fit, and *P*-values were adjusted with the Benjamini–Hochberg method. Genes with adjusted $P < 0.05$ and >2-fold difference between compared groups were identified as significantly different. PCA was performed using the DESeq2 function plotPCA on variance-stabilized expression data (using the DEseq2 function varianceStabilizingTransformation) that was then adjusted for batch, a number of genes detected, and percent uniquely mapped reads for all sample types by subtracting out the DESeq-modeled effects for these variables.

Pathway analysis

We used the PANTHER Gene List Analysis tool (Mi et al., 2019) at http://pantherdb.org to identify overrepresented biological processes within input lists of DE genes by running the statistical overrepresentation test using the complete Gene Ontology Biological Process database. Significantly overrepresented pathways were identified on the basis of Fisher's exact tests with *P*-values corrected by FDR.

RNA-seq deconvolution analysis

We performed deconvolution of variance-stabilized, technical variable-corrected expression data (as used for PCA discussed earlier) on the basis of the LM22 immune cell gene signatures using CIBERSORTx (Newman et al., 2019). Mann–Whitney U tests were performed to determine significant differences in cell proportions between baseline healthy and psoriatic samples. Two-sided Wilcox rank-sum tests were performed to assess patient-matched changes in cell proportions by weeks 2, 4, and 12 of treatment. All tests were performed using the wilcox.test function in R.

Clonotype analysis

MiXCR 3.0.10 (Bolotin et al., 2015) was run on shotgun mode with the −species, hs –starting-material rna, and –only-productive parameters to align raw fastq files for each sample to reference sequences for all TCRs from the international ImMunoGeneTics database (Lefranc et al., 2003) and to further assemble and cluster high-quality TCR-spanning reads into individual TCR sequence clones. We defined a clonotype as a unique combination of V segment, J segment, and CDR3 amino acid sequence and calculated the Inverse Simpson Index using the repDiversity function of the immunarch 0.6.5 R package (ImmunoMind Team, 2019).

Data availability statement

Datasets related to this article can be found at https://www.ncbi.nlm.nih.gov/geo/query/acc.cgi?acc=GSE171012, hosted at Gene Expression Omnibus (Edgar et al., 2002) under the accession number GSE171012.

ORCIDs
Jared Liu: 0000-0001-8481-3129
Hsin-Wen Chang: 0000-0003-2881-245X
Robby Grewal: 0000-0002-0551-2510
Daniel D. Cummins: 0000-0003-3863-153X
Audrey Bui: 0000-0003-3055-463X
Kristen M. Beck: 0000-0002-5342-8356
Sahil Sekhon: 0000-0003-0035-1110
Di Yan: 0000-0003-1338-9847
Zhi-Ming Huang: 0000-0002-8992-1871
Timothy H. Schmidt: 0000-0003-3991-0012
Eric J. Yang: 0000-0002-3763-3309
Isabelle M. Sanchez: 0000-0002-5936-2255
Mio Nakamura: 0000-0002-1367-742X
Shrishti Bhattarai: 0000-0001-8458-336X
Quinn Thibodeaux: 0000-0001-7625-7150
Richard Ahn: 0000-0002-9698-2752
Mariela Pauli: 0000-0002-9180-4789
Tina Bhutani: 0000-0001-8187-1024
Michael D. Rosenblum: 0000-0002-0462-5732
Wilson Liao: 0000-0001-7883-6439

Disclaimer
Novartis had no role in the study conception, design, and data analysis or in the writing of this manuscript.

SUPPLEMENTARY MATERIAL
Supplementary material is linked to the online version of the paper at www.jidonline.org, and at https://doi.org/10.1016/j.xjidi.2021.100094.

REFERENCES

Anders S, Pyl PT, Huber W. HTSeq—a Python framework to work with high-throughput sequencing data. Bioinformatics 2015;31:166−9.

Arakawa A, Siewert K, Stöhr J, Besgen P, Kim SM, Rühl G, et al. Melanocyte antigen triggers autoimmunity in human psoriasis. J Exp Med 2015;212:2203−12.

Bayer AL, Lee JY, de la Barrera A, Surh CD, Malek TR. A function for IL-7R for CD4+ CD25+ Foxp3+ T regulatory cells. J Immunol 2008;181:225−34.

Bolotin DA, Poslavsky S, Mitrophanov I, Shugay M, Mamedov IZ, Putintseva EV, et al. MiXCR: software for comprehensive adaptive immunity profiling. Nat Methods 2015;12:380−1.

Brembilla NC, Stalder R, Senra L, Boehncke WH. IL-17A localizes in the exocytic compartment of mast cells in psoriatic skin. Br J Dermatol 2017;177:1458−60.

Broadley I, Pera A, Morrow G, Davies KA, Kern F. Expansions of cytotoxic CD4$^+$CD28$^-$ T cells drive excess cardiovascular mortality in rheumatoid

arthritis and other chronic inflammatory conditions and are triggered by CMV infection. Front Immunol 2017;8:195.

Chemin K, Gerstner C, Malmström V. Effector functions of CD4+ T cells at the site of local autoimmune inflammation—lessons from rheumatoid arthritis. Front Immunol 2019;10:353.

Cheuk S, Wikén M, Blomqvist L, Nylén S, Talme T, Ståhle M, et al. Epidermal Th22 and Tc17 cells form a localized disease memory in clinically healed psoriasis. J Immunol 2014;192:3111−20.

Chiang CC, Cheng WJ, Korinek M, Lin CY, Hwang TL. Neutrophils in psoriasis. Front Immunol 2019;10:2376.

Colpitts SL, Puddington L, Lefrançois L. IL-15 receptor α signaling constrains the development of IL-17−producing γδ T cells. Proc Natl Acad Sci USA 2015;112:9692−7.

Dobin A, Davis CA, Schlesinger F, Drenkow J, Zaleski C, Jha S, et al. STAR: ultrafast universal RNA-seq aligner. Bioinformatics 2013;29:15−21.

Edgar R, Domrachev M, Lash AE. Gene Expression Omnibus: NCBI gene expression and hybridization array data repository. Nucleic Acids Res 2002;30:207−10.

Halvorsen EH, Strønen E, Hammer HB, Goll GL, Sollid LM, Molberg O. Interleukin-15 induces interleukin-17 production by synovial T cell lines from patients with rheumatoid arthritis. Scand J Immunol 2011;73:243−9.

Harrison OJ, Srinivasan N, Pott J, Schiering C, Krausgruber T, Ilott NE, et al. Epithelial-derived IL-18 regulates Th17 cell differentiation and Foxp3+ Treg cell function in the intestine. Mucosal Immunol 2015;8:1226−36.

Hueber W, Patel DD, Dryja T, Wright AM, Koroleva I, Bruin G, et al. Effects of AIN457, a fully human antibody to interleukin-17A, on psoriasis, rheumatoid arthritis, and uveitis. Sci Transl Med 2010;2:52ra72.

ImmunoMind Team. Immunarch: an R package for painless bioinformatics analysis of T-cell and B-cell immune repertoires. https://doi.org/10.5281/zenodo.3367200; 2019 (accessed December 23, 2020).

Inoue K, Takano H, Shimada A, Satoh M. Metallothionein as an anti-inflammatory mediator. Mediators Inflamm 2009;2009:101659.

Krueger JG, Wharton KA Jr, Schlitt T, Suprun M, Torene RI, Jiang X, et al. IL-17A inhibition by secukinumab induces early clinical, histopathologic, and molecular resolution of psoriasis. J Allergy Clin Immunol 2019;144:750−63.

Lai Y, Li D, Li C, Muehleisen B, Radek KA, Park HJ, et al. The antimicrobial protein REG3A regulates keratinocyte proliferation and differentiation after skin injury. Immunity 2012;37:74−84.

Lande R, Botti E, Jandus C, Dojcinovic D, Fanelli G, Conrad C, et al. The antimicrobial peptide LL37 is a T-cell autoantigen in psoriasis [published correction appears in Nat Commun 2015;6:6595]. Nat Commun 2014;5:5621.

Langley RG, Elewski BE, Lebwohl M, Reich K, Griffiths CE, Papp K, et al. Secukinumab in plaque psoriasis – results of two phase 3 trials. N Engl J Med 2014;371:326−38.

Lebwohl M. Psoriasis. Lancet 2003;361:1197−204.

Lefranc MP, Pommié C, Ruiz M, Giudicelli V, Foulquier E, Truong L, et al. IMGT unique numbering for immunoglobulin and T cell receptor variable domains and Ig superfamily V-like domains. Dev Comp Immunol 2003;27:55−77.

Liu J, Chang HW, Huang ZM, Nakamura M, Sekhon S, Ahn R, et al. Single-cell RNA sequencing of psoriatic skin identifies pathogenic Tc17 cell

subsets and reveals distinctions between CD8+ T cells in autoimmunity and cancer. J Allergy Clin Immunol 2021;147:2370−80.

Love MI, Huber W, Anders S. Moderated estimation of fold change and dispersion for RNA-seq data with DESeq2. Genome Biol 2014;15:550.

Lowes MA, Kikuchi T, Fuentes-Duculan J, Cardinale I, Zaba LC, Haider AS, et al. Psoriasis vulgaris lesions contain discrete populations of Th1 and Th17 T cells. J Invest Dermatol 2008;128:1207−11.

Maehara T, Kaneko N, Perugino CA, Mattoo H, Kers J, Allard-Chamard H, et al. Cytotoxic CD4+ T lymphocytes may induce endothelial cell apoptosis in systemic sclerosis. J Clin Invest 2020;130:2451−64.

Matos TR, O'Malley JT, Lowry EL, Hamm D, Kirsch IR, Robins HS, et al. Clinically resolved psoriatic lesions contain psoriasis-specific IL-17-producing αβ T cell clones. J Clin Invest 2017;127:4031−41.

Mi H, Muruganujan A, Ebert D, Huang X, Thomas PD. PANTHER version 14: more genomes, a new Panther GO-slim and improvements in enrichment analysis tools. Nucleic Acids Res 2019;47:D419−26.

Newman AM, Steen CB, Liu CL, Gentles AJ, Chaudhuri AA, Scherer F, et al. Determining cell type abundance and expression from bulk tissues with digital cytometry. Nat Biotechnol 2019;37:773−82.

Nussbaum L, Chen YL, Ogg GS. Role of regulatory T cells in psoriasis pathogenesis and treatment. Br J Dermatol 2021;184:14−24.

Ortega C, Fernández-A S, Carrillo JM, Romero P, Molina IJ, Moreno JC, et al. IL-17-producing CD8+ T lymphocytes from psoriasis skin plaques are cytotoxic effector cells that secrete Th17-related cytokines. J Leukoc Biol 2009;86:435−43.

Reich K, Papp KA, Matheson RT, Tu JH, Bissonnette R, Bourcier M, et al. Evidence that a neutrophil-keratinocyte crosstalk is an early target of IL-17A inhibition in psoriasis. Exp Dermatol 2015;24:529−35.

Sanchez Rodriguez R, Pauli ML, Neuhaus IM, Yu SS, Arron ST, Harris HW, et al. Memory regulatory T cells reside in human skin. J Clin Invest 2014;124:1027−36.

Sugiyama H, Gyulai R, Toichi E, Garaczi E, Shimada S, Stevens SR, et al. Dysfunctional blood and target tissue CD4+CD25high regulatory T cells in psoriasis: mechanism underlying unrestrained pathogenic effector T cell proliferation. J Immunol 2005;174:164−73.

Teunissen MB, Koomen CW, de Waal Malefyt R, Wierenga EA, Bos JD. Interleukin-17 and interferon-gamma synergize in the enhancement of proinflammatory cytokine production by human keratinocytes. J Invest Dermatol 1998;111:645−9.

Villadsen LS, Schuurman J, Beurskens F, Dam TN, Dagnaes-Hansen F, Skov L, et al. Resolution of psoriasis upon blockade of IL-15 biological activity in a xenograft mouse model. J Clin Invest 2003;112:1571−80.

Waickman AT, Keller HR, Kim TH, Luckey MA, Tai X, Hong C, et al. The cytokine receptor IL-7Rα impairs IL-2 receptor signaling and constrains the in vitro differentiation of Foxp3+ Treg cells. iScience 2020;23:101421.

Zhang XJ, Yan KL, Wang ZM, Yang S, Zhang GL, Fan X, et al. Polymorphisms in interleukin-15 gene on chromosome 4q31.2 are associated with psoriasis vulgaris in Chinese population. J Invest Dermatol 2007;127:2544−51.